1.5.2 Physical Parameters of Perovskite Light-Emitting Diodes

Similar to conventional LEDs, the performance of a PeLED can be evaluated based on several physical parameters such as turn-on voltage, brightness or irradiance, peak luminous half-wave width (FWHM), EQE, current efficiency, lumen efficiency, energy conversion efficiency, and stability.

The turn-on voltage is the voltage at which the device starts to operate at a certain level of brightness, typically 1 cd m^{-2} for visible LEDs or when it starts to exhibit an EQE for UV or IR LEDs. The brightness, or irradiance, is the intensity of radiation emitted by the device, measured in cd m^{-2} or W sr^{-1} m^{-2}. The required brightness levels will depend on the intended application of the LED.

The peak-half-peak width of the luminous spectrum represents the purity of the emitted light. A narrower FWHM indicates a purer luminous color, which is desirable for display applications.

EQE is an important measure of light-emitting devices and is defined as the ratio of the number of photons emitted per unit time to the number of electrons injected. It can also be described by the following Eq. (1.4).

$$EQE = f_{\text{balance}} \times f_{\text{e-h}} \times \eta_{\text{radiative}} \times f_{\text{outcoupling}} \tag{1.4}$$

where f_{balance} is the equilibrium charge injection probability (which has a value of 1 when the number of electrons and holes injected is the same), $f_{\text{e-h}}$ is the probability of each carrier pair forming an electron–hole pair or exciton, $\eta_{\text{radiative}}$ is the probability of each electron–hole pair radiating a composite, and $f_{\text{outcoupling}}$ is the optical output coupling rate.

In order to enhance the luminescence efficiency, certain conditions need to be met, including maintaining a balance of electron and hole injection, increasing the chance of electron–hole pair formation, maximizing the ratio of the radiation composite to non-radiation composite, and effectively coupling the generated photons within the luminescent layer to the output. The balance of charge injection in the LED depends on the injection potential of electrons and holes into the perovskite conduction and valence bands, as well as the mobility of electrons and holes, which are limited by the type and properties of the transport layer material. The rate of electron–hole pair formation and combination efficiency can be regarded as the internal quantum efficiency of the material, which is related to material properties such as exciton binding energy and defect density of states. The efficiency of light coupling output mainly depends on the device structure and is subject to the refractive index and shape of the device layers. Typically, the planar structure of an LED limits the light-coupling efficiency to 25%, with most of the photon energy being dissipated in the form of a light waveguide within the device.

Current efficiency is the luminance of the light-emitting device and the ratio of current in cd A^{-1}; lumen efficiency is the ratio of the luminous flux emitted by the device to the electrical power input in lm W^{-1}; and energy conversion efficiency is the ratio of the photon energy emitted by the device to the total energy input.

Stability refers to the operating lifespan of an LED, which is typically measured by the time it takes for the device's brightness or EQE to decay to half of its initial value

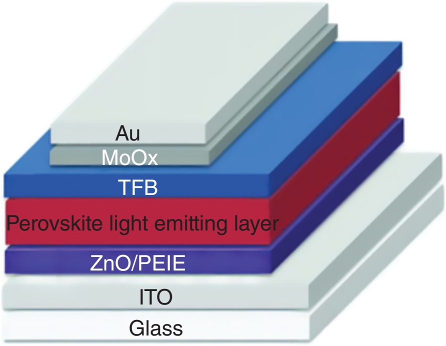

Figure 1.14 Structure diagram of a perovskite light-emitting diode device with ZnO/PEIE as the electron injection layer and TFB as the hole injection layer. Source: Stranks et al. [72]/John Wiley & Sons/CC BY 4.0.

at a constant voltage or current, also known as T50. There are also other measures, such as T90 and T80, which indicate the time taken for the brightness or EQE to decay to 90% and 80% of its initial value, respectively. Devices with better stability are more desirable for commercialization purposes.

Figure 1.14 illustrates the structure of a typical PeLED device. The perovskite light-emitting layer is sandwiched between the electron injection layer ZnO/PEIE and the hole injection layer TFB. When an external electric field is applied, electrons and holes are injected from the electron injection layer and hole injection layer, respectively, and they recombine in the perovskite layer, emitting light. To enhance the efficiency of electron injection, the electron affinity of the electron injection layer can be reduced. For example, doping Mg can form a ZnMgO structure in ZnO, leading to enhanced electron injection efficiency [100, 101]. Alternatively, an additional interface layer, such as polyethyleneimine, can be added between the injection layer and the light-emitting layer to improve electron injection. Similarly, the hole injection barrier can be reduced by doping the hole injection layer with perfluorinated lithium ion salt or by incorporating hole-transporting materials with high HOMO (highest occupied molecular orbital) energy levels, such as 4,4′-bis(9-carbazole) biphenyl, to lower the hole injection barrier [40, 102, 103].

The injection potentials of different layers can be determined by UV photoelectron spectroscopy. However, the energy level structure of perovskites is affected by the substrate work function, which means that UV photoelectron spectroscopy of perovskites requires the film to be deposited on a substrate that closely mimics the device structure. Alternatively, electron absorption spectroscopy can be used to measure the injection barrier in the device [104]. In electron absorption spectroscopy, the effect of the internal electric field on the transmitted light is mainly measured [105]. According to the single-electron Franz–Keldysh–Aspnes low electric field theory, the transmitted light varies with the square of the electric field, which can also be applied to $MAPbI_3$ and other bulk materials [106, 107]. The magnitude of the internal electric field can be measured by modulating the internal electric field with a DC bias. However, the effect of ion shielding has to be taken into account in this process [108].

1.5.3 Device Performance Development of Perovskite Light-Emitting Diodes

In summary, the luminescence and physical properties of perovskite are influenced by several factors. These include the crystal structure of the perovskite, size effects, radiative and non-radiative processes of photons, interface states, and charge injection balance.

In most PeLEDs, the EQE and light output tend to decrease as the current density (J) increases, primarily due to augmented Auger recombination, Joule heating, or imbalanced charge injection. This EQE roll-off phenomenon is also observed in other LED technologies (Figure 1.15b) and typically leads to a 50% decrease in EQE when J ranges from 100 to 1000 mA cm^{-2}. Only a limited number of devices have reported EQE values above 1 A cm^{-2}, and these devices are typically fabricated using pure-phase 2D or mixed-phase 2D/3D perovskite materials (Figure 1.15c). Significantly, PeLEDs with reduced EQE roll-off exhibit low turn-on voltages (V_{ON}), indicating barrier-free charge transport/injection. A low driving voltage can also help alleviate the quantum-confined Stark effect, which is another potential cause for EQE roll-off [11].

Changes in the dimensionality and crystal defects of the perovskite affect the state of the exciton and carrier transport, resulting in a significant change in device performance. In two-dimensional and one-dimensional perovskites, the exciton binding energy is stronger, resulting in a wider color gamut. In contrast, three-dimensional perovskites have a weaker exciton binding energy, leading to a narrower color spectrum. Crystal defects impact the carrier transport capacity, and higher defect densities lead to more exciton capture, resulting in more non-radiative output and reduced device efficiency.

Radiative and non-radiative processes of photons are closely linked to the crystal structure, size effects, exciton binding energy, and trap density, influencing the combination path of excitons. Excitation light density also affects radiation and decay processes. Surface and interface trap states significantly influence non-radiative processes, and surface state modulation can improve device luminous efficiency. Charge injection balance mainly depends on the energy level structure of the material layers and the ideal balance of injection potential at the interface, ensuring both stable device operation and improved EQE.

Although PeLED research started later than that of perovskite solar cells, it has experienced significant development in a short period. In just a few years, the EQE of PeLEDs has increased from less than 0.1% to over 20% [110–114]. To date, the maximum EQEs for near-infrared, red, green, blue, and white light-emitting perovskite diodes have reached 25.5%, 25.8%, 30.84%, 18.65%, and 12.2%, respectively [115–119] (Figure 1.16).

Figure 1.17a presents a comparison of the color gamut of LFMHP-based LEDs, demonstrating that the blue and red components have already fulfilled the requirements of the Rec. 2020 standard, while the green component still requires further improvement. Another critical factor limiting the commercialization of PeLEDs is device lifetime. Figure 1.17b illustrates the promising device stability

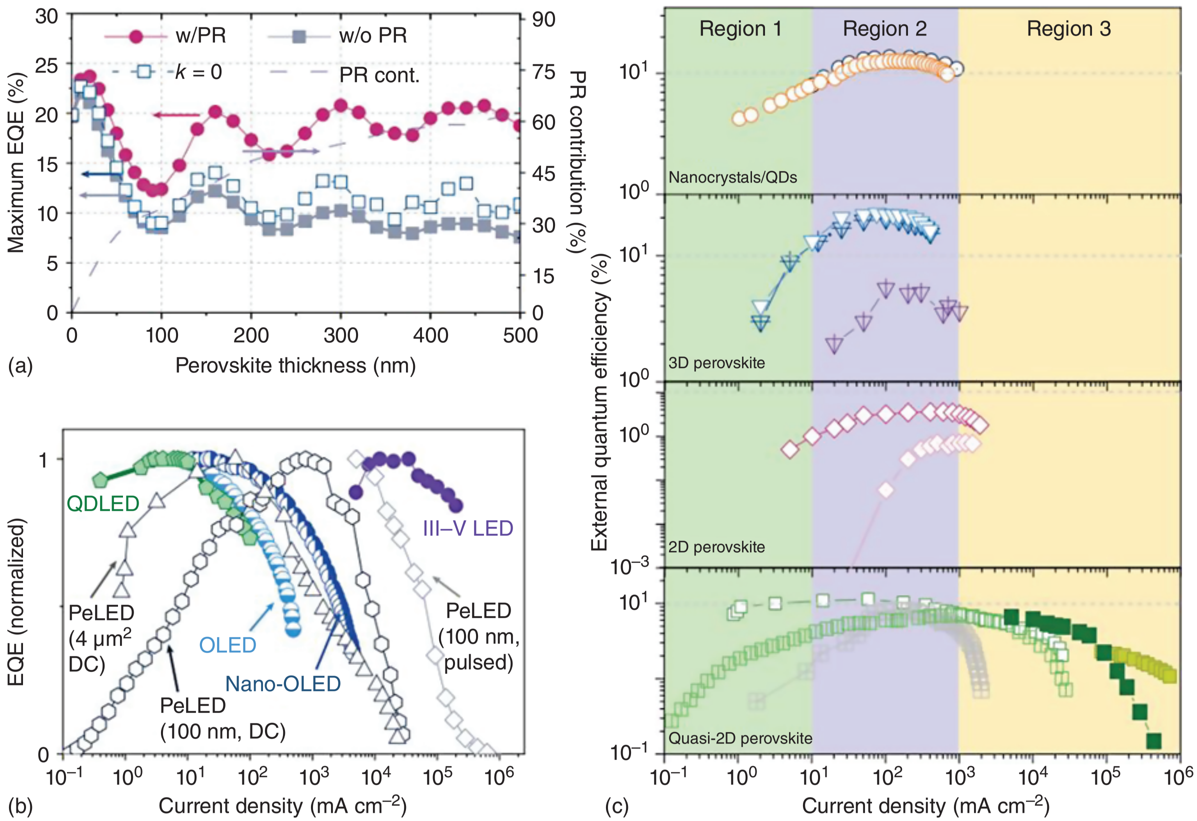

Figure 1.15 Photon-recycling and EQE roll-off in PeLEDs. (a) Calculated EQEs with and without photon recycling (PR; filled red circles and filled gray squares, respectively) and without reabsorption (open navy blue squares), as well as the relative photon recycling contribution (violet dashed lines) for an ideal PeLED (IQE = 100%) with perovskite EMLs of various thickness. *k* indicates the refractive index component connected to the absorption coefficient. Source: Cho et al. [109]/Springer Nature/CC BY 4.0. (b) A comparison of EQE roll-off in various thin-film LEDs (organic LEDs, OLEDs and nano-OLEDs, QDLEDs, and PeLEDs with state-of-the-art crystalline III–V LEDs). DC, direct current. LEDs are biased via steady-state voltage. Source: Fakharuddin et al. [11]/Springer Nature. (c) EQE roll-off trends of some notable PeLEDs reported in the literature employing NCs, 3D, 2D, and 2D/3D EMLs. The plot is divided into three regions based on injection current densities and the type of EML. Source: Fakharuddin et al. [11]/Springer Nature.

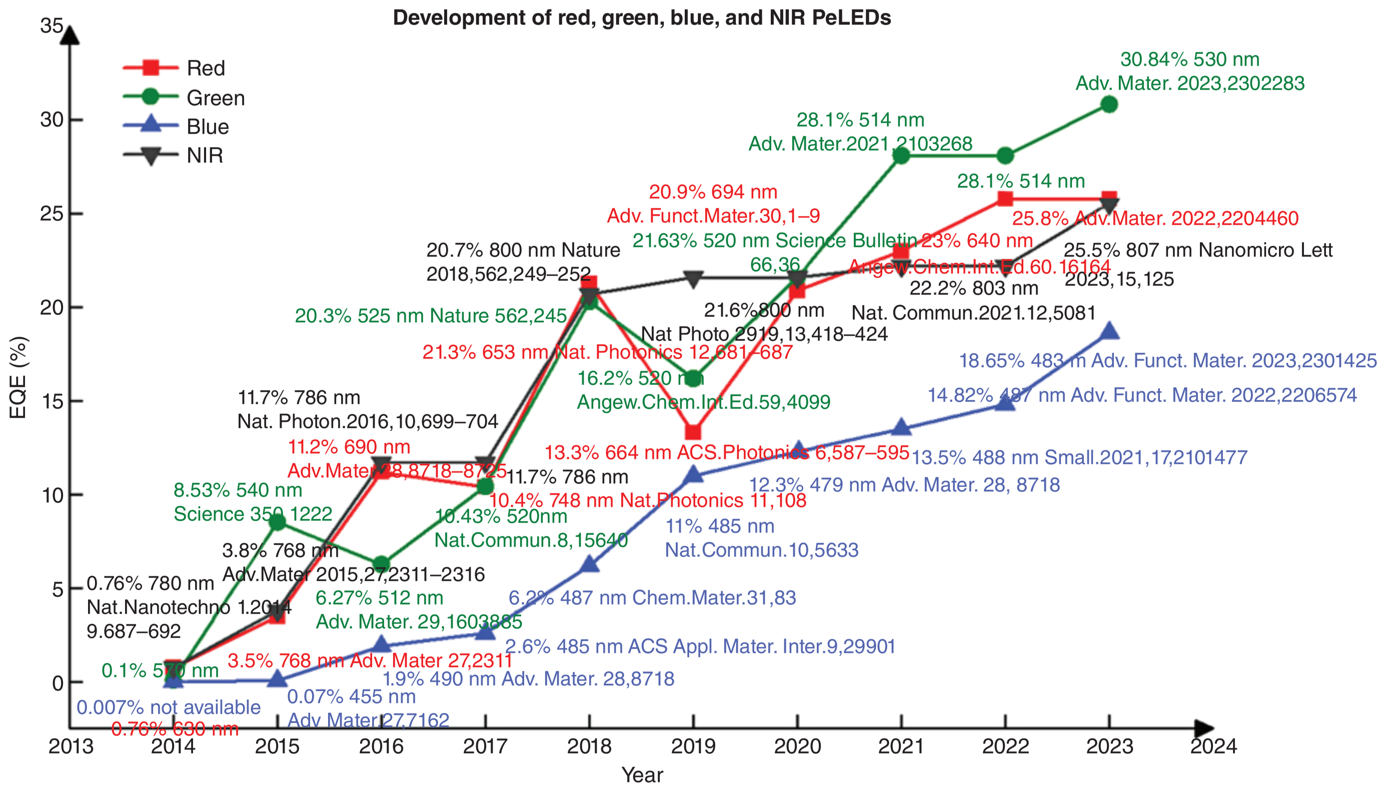

Figure 1.16 The development in EQEs of red, green, blue, and NIR PeLEDs.

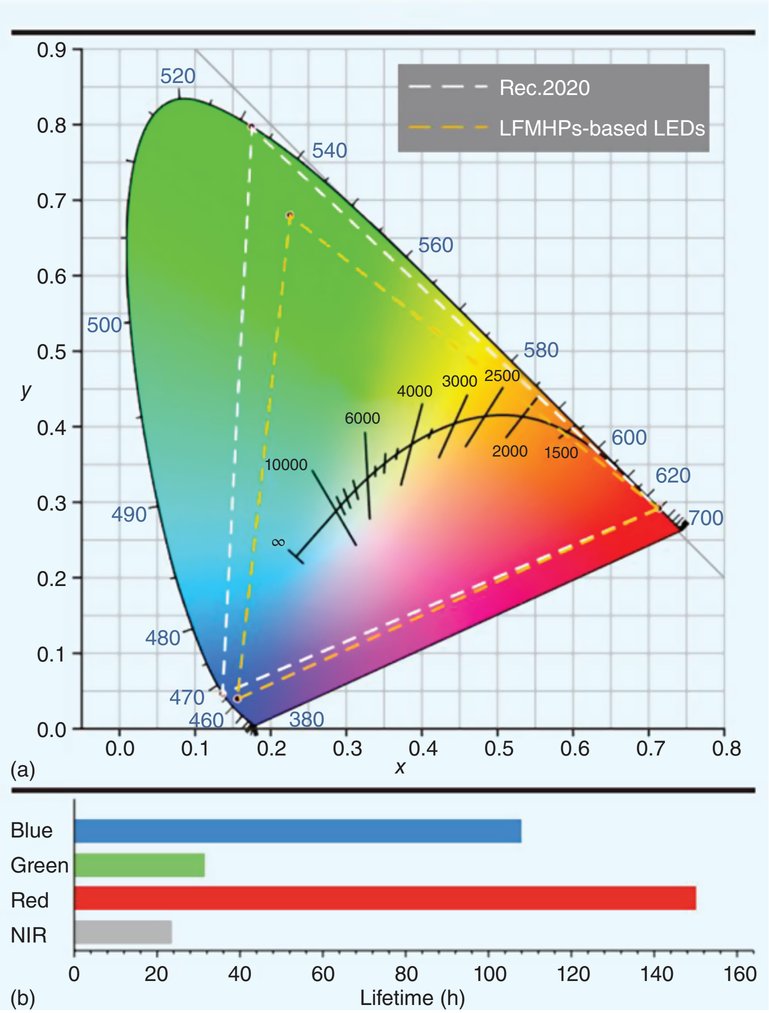

Figure 1.17 Current status of perovskite light-emitting diodes (PeLEDs) based on lead-free metal halide perovskite (LFMHP) emitters. (a) Color gamut coverage of Rec. 2020 and LFMHP-based PeLEDs. (b) Device lifetime of state-of-the-art NIR, red, green, and blue-emitting LFMHP-based PeLEDs. Source: Wang et al. [120]/Innovation Press Co., Limited.

of LFMHP-based LEDs, indicating their potential in overcoming the inherent chemical instability issue found in LHP-based LEDs [120].

1.6 Summary

Perovskite materials are highly sought after for their luminescent properties, including their ability to emit light when excited by an external energy source. This luminescence is due to the presence of a bandgap in the electronic structure of the material, which allows for the absorption and re-emission of light. This chapter discusses the structure and luminescent properties of perovskite materials, as well as some important physical parameters of PeLEDs and their current development status.

Metal halide perovskites, composed of a lead or tin cation, a halide anion (such as iodide or bromide), and an organic or inorganic A-site cation (such as methylammonium or cesium), are an important class of perovskite materials for optoelectronic applications. These materials exhibit high defect tolerance, which means they can accommodate a high density of defects and impurities without significantly degrading their electronic and optical properties. Metal halide perovskites exhibit a range of luminescent properties, including strong photoluminescence (PL) and electroluminescence (EL) across the visible spectrum. The crystal structure and composition of the material, as well as the presence of defects and impurities, strongly influence their PL and EL properties.

Perovskite LEDs have the potential to operate under ultra-high brightness conditions, allowing for the passage of high currents ($100\,\mathrm{cm}^2\ \mathrm{V}^{-1}\mathrm{S}^{-1}$ or higher) through the diode without causing detrimental processes. This provides an advantage over organic and colloidal quantum dot semiconductors in high-brightness operations. Peak brightness exceeding $10^5\,\mathrm{cd\,m}^{-2}$ has been achieved [96], and a recent encouraging aging report using two-dimensional perovskites in LEDs demonstrated no significant degradation in device operation at a current density of $\mathrm{A\,cm}^{-2}$ [121].

However, the high-brightness operation of perovskite LEDs is currently hindered by other factors, including the instability of ionic materials under an electric field (ionic migration) [122], imbalanced carrier injection, and non-radiative and Auger recombination losses that occur mainly under low/high injection conditions [123]. These factors may further contribute to the degradation associated with heating.

Perovskite materials also show promise for other applications, such as solar cells, LEDs, lasers, and sensors. Their unique combination of properties, including high defect tolerance, tunable bandgap, and excellent charge transport properties, makes them an attractive candidate for a wide range of optoelectronic applications. Perovskite materials have also been explored for use in sensors, particularly for detecting gases and ions, due to their unique electronic properties, high surface area, and ability to selectively bind to certain molecules.

However, perovskite materials have some challenges that need to be addressed before they can be widely deployed in commercial applications. Their instability in the presence of moisture and oxygen can lead to degradation over time, which is a major obstacle for the development of perovskite-based solar cells. Researchers have made progress in addressing this issue through the development of encapsulation strategies and the use of stable electrode materials, but further work is needed to improve long-term stability. The toxicity of some of the elements used in perovskite materials, particularly lead, is another challenge. While there has been progress in developing lead-free perovskites, many of these materials have lower performance than their lead-based counterparts.

Furthermore, PeLEDs still face challenges in terms of the poor efficiency of blue devices, a decline in EQE under high-brightness conditions, and insufficient device lifespans. The low efficiency of blue PeLEDs is often attributed to halide segregation in mixed Cl–Br perovskite emitters. Some progress has been made through compositional adjustments and the incorporation of bulky organic cations in low-dimensional perovskites. Large organic cations can stiffen the perovskite crystal structure, reducing detrimental electron–phonon interactions and ion migration. However, these cations are typically insulating, resulting in inferior charge transport and reduced device performance. One potential solution is to replace these insulating ligands, commonly alkyl-chained, with conjugated semiconducting ligands, which could potentially alleviate this issue [11].

EQE roll-off and operational stability are significant challenges for PeLEDs, influenced by both intrinsic factors of the perovskite active layer and extrinsic parameters of the device. Ongoing strategies to address these challenges include compositional and dimensional engineering of the perovskite emitter, formation of defect-free emissive layers (EMLs) through passivation techniques, optimization of heterointerfaces to enable barrier-free charge transport and injection, achieving balanced charge injection, operating the devices at low voltages, and reducing the transport resistance in the emissive layer. Given the ionic nature of halide perovskites, the development of specific biasing schemes (e.g. pulsed biasing) may assist in minimizing ion migration and enhancing stability [11].

There is also a need for more research on the potential environmental impact of large-scale perovskite production and deployment, as well as the scalability and reproducibility of perovskite synthesis and device fabrication.

Despite these challenges, perovskite materials hold tremendous potential for a range of applications, and the field is likely to see continued rapid development and progress in the coming years. Advances in perovskite synthesis and device engineering have led to significant improvements in performance, and it is likely that perovskites will continue to be a focus of research and development. Further improvements in performance and stability, as well as the development of new applications and markets for perovskite materials, are expected as continued research and development in this area progresses.

References

1 You, Y.M., Liao, W.Q., Zhao, D. et al. (2017). An organic-inorganic perovskite ferroelectric with large piezoelectric response. *Science* 357: 306–309.

2 Møller, C.K. (1958). Crystal structure and photoconductivity of caesium plumbohalides. *Nature* 182: 1436–1436.

3 Bansal, V., Poddar, P., Ahmad, A. et al. (2006). Room-temperature biosynthesis of ferroelectric barium titanate nanoparticles. *Journal of the American Chemical Society* 128: 11958–11963.

4 Bednorz, J.G. and Müller, K.A. (1986). Possible high Tc superconductivity in the Ba-La-Cu-O system. *Zeitschrift für Physik B Condensed Matter* 64: 189–193.

5 Jin, S., Tiefel, T.H., McCormack, M. et al. (1994). Thousandfold change in resistivity in magnetoresistive La-Ca-Mn-O films. *Science* 264: 413–415.

6 Miao, X., Zhang, L., Wu, L. et al. (2019). Quadruple perovskite ruthenate as a highly efficient catalyst for acidic water oxidation. *Nature Communications* 10: 1–7.

7 Zhao, Y.C., Zhou, W.K., Zhou, X. et al. (2017). Quantification of light-enhanced ionic transport in lead iodide perovskite thin films and its solar cell applications. *Light: Science & Applications* 6: 16243–16243.

8 Mitzi, D.B. (2001). Thin-film deposition of organic-inorganic hybrid materials. *Chemistry of Materials* 13: 3283–3298.

9 Quan, L.N., Garcia de Arquer, F.P., Sabatini, R.P. et al. (2018). Perovskites for light emission. *Advanced Materials* 30: 1801996.

10 Kojima, A., Teshima, K., Shirai, Y. et al. (2009). Organometal halide perovskites as visible-light sensitizers for photovoltaic cells. *Journal of the American Chemical Society* 131: 6050–6051.

11 Fakharuddin, A., Gangishetty, M.K., Abdi-Jalebi, M. et al. (2022). Perovskite light-emitting diodes. *Nature Electronics* 5: 203–216.

12 Kang, J. and Wang, L.W. (2017). High defect tolerance in lead halide perovskite $CsPbBr_3$. *The Journal of Physical Chemistry Letters* 8: 489–493.

13 Yettapu, G.R., Talukdar, D., Sarkar, S. et al. (2016). Terahertz conductivity within colloidal $CsPbBr_3$ perovskite nanocrystals: remarkably high carrier mobilities and large diffusion lengths. *Nano Letters* 16: 4838–4848.

14 Shi, D., Adinolfi, V., Comin, R. et al. (2015). Low trap-state density and long carrier diffusion in organolead trihalide perovskite single crystals. *Science* 347: 519–522.

15 Brandt, R.E., Stevanović, V., Ginley, D.S. et al. (2015). Identifying defect-tolerant semiconductors with high minority-carrier lifetimes: beyond hybrid lead halide perovskites. *MRS Communications* 5: 265–275.

16 Mesquita, I., Andrade, L., and Mendes, A. (2018). Perovskite solar cells: materials, configurations and stability. *Renewable and Sustainable Energy Reviews* 82: 2471–2489.

17 Liu, A., Bi, C., Guo, R. et al. (2021). Electroluminescence principle and performance improvement of metal halide perovskite light-emitting diodes. *Advanced Optical Materials* 9.

18 Zhao, C., Zhang, D., and Qin, C. (2020). Perovskite light-emitting diodes. *CCS Chemistry* 2: 859–869.

19 Cheng, H., Feng, Y., Fu, Y. et al. (2022). Understanding and minimizing non-radiative recombination losses in perovskite light-emitting diodes. *Journal of Materials Chemistry C* 10: 13590–13610.

20 Shi, Z., Li, Y., Zhang, Y. et al. (2017). High-efficiency and air-stable perovskite quantum dots light-emitting diodes with an all-inorganic heterostructure. *Nano letters* 17: 313–321.

21 Han, B., Cai, B., Shan, Q. et al. (2018). Stable, efficient red perovskite light-emitting diodes by (α, δ)-$CsPbI_3$ phase engineering. *Advanced Functional Materials* 28: 1804285.

22 Ban, M., Zou, Y., Rivett, J.P.H. et al. (2018). Solution-processed perovskite light emitting diodes with efficiency exceeding 15% through additive-controlled nanostructure tailoring. *Nature Communications* 9: 1–10.

23 Protesescu, L., Yakunin, S., Kumar, S. et al. (2017). Dismantling the "red wall" of colloidal perovskites: highly luminescent formamidinium and formamidinium-cesium lead iodide nanocrystals. *ACS Nano* 11: 3119–3134.

24 Schweinberger, F.F., Berr, M.J., Doblinger, M. et al. (2013). Cluster size effects in the photocatalytic hydrogen evolution reaction. *Journal of the American Chemical Society* 135: 13262–13265.

25 Dresselhaus (2022). *Optical Properties of Solids*. Oxford University Press.

26 Zhu, X.Y. and Podzorov, V. (2015). Charge carriers in hybrid organic inorganic lead halide perovskites might be protected as large polarons. *The Journal of Physical Chemistry Letters* 6: 4758–4761.

27 Smith, M.D. and Karunadasa, H.I. (2018). White light emission from layered halide perovskites. *Accounts of Chemical Research* 51: 619–627.

28 Tokizaki, T., Makimura, T., Akiyama, H. et al. (1991). Femtosecond cascade-excitation spectroscopy for nonradiative deexcitation and lattice relaxation of the self-trapped exciton in NaCl. *Physical Review Letters* 67: 2701–2704.

29 Zhang, L., Sun, C., He, T. et al. (2021). High-performance quasi-2D perovskite light-emitting diodes: from materials to devices. *Light: Science & Applications* 10: 61.

30 Efros, A.L., Rosen, M., Kuno, M. et al. (1996). Band-edge exciton in quantum dots of semiconductors with a degenerate valence band: dark and bright exciton states. *Physical Review B* 54: 4843–4856.

31 Franceschetti, A., Fu, H., Wang, L.W. et al. (1999). Many-body pseudopotential theory of excitons in InP and CdSe quantum dots. *Physical Review B* 60: 1819–1829.

32 Leung, K., Pokrant, S., and Whaley, K.B. (1998). Exciton fine structure in CdSe nanoclusters. *Physical Review B* 57: 12291–12301.

33 Crooker, S.A., Barrick, T., Hollingsworth, J.A. et al. (2003). Multiple temperature regimes of radiative decay in CdSe nanocrystal quantum dots: intrinsic limits to the dark-exciton lifetime. *Applied Physics Letters* 82: 2793–2795.

34 Labeau, O., Tamarat, P., and Lounis, B. (2003). Temperature dependence of the luminescence lifetime of single CdSe/ZnS quantum dots. *Physical Review Letters* 90: 257404.

35 Donegá, C.M., Bode, M., and Meijerink, M. (2006). Size- and temperature-dependence of exciton lifetimes in CdSe quantum dots. *Physical Review B* 74: 085320.

36 Wang, H., Donegá, C.M., Meijerink, A. et al. (2006). Ultrafast exciton dynamics in CdSe quantum dots studied from bleaching recovery and fluorescence transients. *The Journal of Physical Chemistry B* 110: 733–737.

37 Zhao, Q., Peter, A., Wesley, B.J. et al. (2007). Shape dependence of band-edge exciton fine structure in CdSe nanocrystals. *Nano Letters* 7: 3274–3280.

38 Oron, D., Aharoni, A., Donega, C.M. et al. (2009). Universal role of discrete acoustic phonons in the low-temperature optical emission of colloidal quantum dots. *Physical Review Letters* 102: 177402.

39 Schaller, R.D., Crooker, S.A., Bussian, D.A. et al. (2010). Revealing the exciton fine structure of PbSe nanocrystal quantum dots using optical spectroscopy in high magnetic fields. *Physical Review Letters* 105: 067403.

40 Veldhuis, S.A., Boix, P.P., Yantara, N. et al. (2016). Perovskite materials for light-emitting diodes and lasers. *Advanced Materials* 28: 6804–6834.

41 Vasilopoulou, M., Fakharuddin, A., García de Arquer, F.P. et al. (2021). Advances in solution-processed near-infrared light-emitting diodes. *Nature Photonics* 15: 656–669.

42 Richter, J.M., Abdi-Jalebi, M., Sadhanala, A. et al. (2016). Enhancing photoluminescence yields in lead halide perovskites by photon recycling and light out-coupling. *Nature Communications* 7: 13941.

43 Lin, Q., Armin, A., Nagiri, R.C. et al. (2014). Electro-optics of perovskite solar cells. *Nature Photonics* 9: 106–112.

44 Saba, M., Cadelano, M., Marongiu, D. et al. (2014). Correlated electron-hole plasma in organometal perovskites. *Nature Communications* 5: 5049.

45 Deschler, F., Price, M., Pathak, S. et al. (2014). High photoluminescence efficiency and optically pumped lasing in solution-processed mixed halide perovskite semiconductors. *The Journal of Physical Chemistry Letters* 5: 1421–1426.

46 Wang, H., Zhang, X., Wu, Q. et al. (2019). Trifluoroacetate induced small-grained $CsPbBr_3$ perovskite films result in efficient and stable light-emitting devices. *Nature Communications* 10: 665.

47 Tan, Z.K., Moghaddam, R.S., Lai, M.L. et al. (2014). Bright light-emitting diodes based on organometal halide perovskite. *Nature Nanotechnology* 9: 687–692.

48 Congreve, D.N., Weidman, M.C., Seitz, M. et al. (2017). Tunable light-emitting diodes utilizing quantum-confined layered perovskite emitters. *ACS Photonics* 4: 476–481.

49 Li, G., Tan, Z.K., Di, D. et al. (2015). Efficient light-emitting diodes based on nanocrystalline perovskite in a dielectric polymer matrix. *Nano Letters* 15: 2640–2644.

50 Hutter, E.M., Gelvez-Rueda, M.C., Osherov, A. et al. (2017). Direct-indirect character of the bandgap in methylammonium lead iodide perovskite. *Nature Materials* 16: 115–120.

51 Etienne, T., Mosconi, E., and De Angelis, F. (2016). Dynamical origin of the Rashba effect in organohalide lead perovskites: a key to suppressed carrier recombination in perovskite solar cells? *The Journal of Physical Chemistry Letters* 7: 1638–1645.

52 Davies, C.L., Filip, M.R., Patel, J.B. et al. (2018). Bimolecular recombination in methylammonium lead triiodide perovskite is an inverse absorption process. *Nature Communications* 9: 293.

53 Niesner, D., Wilhelm, M., Levchuk, I. et al. (2016). Giant Rashba splitting in $CH_3NH_3PbBr_3$ organic-inorganic perovskite. *Physical Review Letters* 117: 126401.

54 Isarov, M., Tan, L.Z., Bodnarchuk, M.I. et al. (2017). Rashba effect in a single colloidal $CsPbBr_3$ perovskite nanocrystal detected by magneto-optical measurements. *Nano Letters* 17: 5020–5026.

55 Stroppa, A., Di Sante, D., Barone, P. et al. (2014). Tunable ferroelectric polarization and its interplay with spin-orbit coupling in tin iodide perovskites. *Nature Communications* 5.

56 March, S.A., Riley, D.B., Clegg, C. et al. (2017). Four-wave mixing in perovskite photovoltaic materials reveals long dephasing times and weaker many-body interactions than GaAs. *ACS Photonics* 4: 1515–1521.

57 Elkins, M.H., Pensack, R., Proppe, A.H. et al. (2017). Biexciton resonances reveal exciton localization in stacked perovskite quantum wells. *The Journal of Physical Chemistry Letters* 8: 3895–3901.

58 Richter, J.M., Branchi, F., de Almeida Camargo, F.V. et al. (2017). Ultrafast carrier thermalization in lead iodide perovskite probed with two-dimensional electronic spectroscopy. *Nature Communications* 8: 376.

59 Price, M.B., Butkus, J., Jellicoe, T.C. et al. (2015). Hot-carrier cooling and photoinduced refractive index changes in organic-inorganic lead halide perovskites. *Nature Communications* 6: 8420.

60 Yang, J., Wen, X., Xia, H. et al. (2017). Acoustic-optical phonon up-conversion and hot-phonon bottleneck in lead-halide perovskites. *Nature Communications* 8: 14120.

61 Yang, Y., Ostrowski, D.P., France, R.M. et al. (2015). Observation of a hot-phonon bottleneck in lead-iodide perovskites. *Nature Photonics* 10: 53–59.

62 Chang, A.Y., Cho, Y.J., Chen, K.C. et al. (2016). Slow organic-to-inorganic sub-lattice thermalization in methylammonium lead halide perovskites observed by ultrafast photoluminescence. *Advanced Energy Materials* 6: 1600422.

63 Stranks, S.D., Burlakov, V.M., Leijtens, T. et al. (2014). Recombination kinetics in organic-inorganic perovskites: excitons, free charge, and subgap states. *Physical Review Applied* 2: 034007.

64 Chondroudis, K. and Mitzi, D.B. (1999). Electroluminescence from an organic-inorganic perovskite incorporating a quaterthiophene dye within lead halide perovskite layers. *Chemistry of Materials* 11: 3028–3030.

65 Wu, X., Trinh, M.T., Niesner, D. et al. (2015). Trap states in lead iodide perovskites. *Journal of the American Chemical Society* 137: 2089–2096.

66 Xiao, Z., Kerner, R.A., Zhao, L. et al. (2017). Efficient perovskite light-emitting diodes featuring nanometre-sized crystallites. *Nature Photonics* 11: 108–115.

67 Yuan, M., Quan, L.N., Comin, R. et al. (2016). Perovskite energy funnels for efficient light-emitting diodes. *Nature Nanotechnology* 11: 872–877.

68 Quan, L.N., Zhao, Y., Garcia de Arquer, F.P. et al. (2017). Tailoring the energy landscape in quasi-2D halide perovskites for efficient light emission. *Nano Letters* 17: 3701–3709.

69 Pan, J., Quan, L.N., Zhao, Y. et al. (2016). Highly efficient perovskite-quantum-dot light-emitting diodes by surface engineering. *Advanced Materials* 28: 8718–8725.

70 Milot, R.L., Sutton, R.J., Eperon, G.E. et al. (2016). Charge-carrier dynamics in 2D hybrid metal-halide perovskites. *Nano Letters* 16: 7001–7007.

71 Yang, Y., Yang, M., Li, Z. et al. (2015). Comparison of recombination dynamics in $CH_3NH_3PbBr_3$ and $CH_3NH_3PbI_3$ perovskite films: influence of exciton binding energy. *The Journal of Physical Chemistry Letters* 6: 4688–4692.

72 Stranks, S.D., Hoye, R.L., Di, D. et al. (2019). The physics of light emission in halide perovskite devices. *Advanced Materials* 31: 1803336.

73 Stranks, S.D. and Snaith, H.J. (2015). Metal-halide perovskites for photovoltaic and light-emitting devices. *Nature Nanotechnology* 10: 391–402.

74 Green, M.A., Ho-Baillie, A., and Snaith, H.J. (2014). The emergence of perovskite solar cells. *Nature Photonics* 8: 506–514.

75 De Wolf, S., Holovsky, J., Moon, S.J. et al. (2014). Organometallic halide perovskites: sharp optical absorption edge and its relation to photovoltaic performance. *The Journal of Physical Chemistry Letters* 5: 1035–1039.

76 Sadhanala, A., Deschler, F., Thomas, T.H. et al. (2014). Preparation of single-phase films of $CH_3NH_3Pb(I_{1-x}Br_x)_3$ with sharp optical band edges. *The Journal of Physical Chemistry Letters* 5: 2501–2505.

77 Abdi-Jalebi, M., Andaji-Garmaroudi, Z., Cacovich, S. et al. (2018). Maximizing and stabilizing luminescence from halide perovskites with potassium passivation. *Nature* 555: 497–501.

78 Stranks, S.D. (2017). Nonradiative losses in metal halide perovskites. *ACS Energy Letters* 2: 1515–1525.

79 Wehrenfennig, C., Eperon, G.E., Johnston, M.B. et al. (2014). High charge carrier mobilities and lifetimes in organolead trihalide perovskites. *Advanced Materials* 26: 1584–1589.

80 Draguta, S., Thakur, S., Morozov, Y.V. et al. (2016). Spatially non-uniform trap state densities in solution-processed hybrid perovskite thin films. *The Journal of Physical Chemistry Letters* 7: 715–721.

81 Wu, C., Wu, T., Yang, Y. et al. (2019). Alternative type two-dimensional-three-dimensional lead halide perovskite with inorganic sodium ions as a spacer for high-performance light-emitting diodess. *ACS Nano* 13: 1645–1654.

82 Meng, F., Liu, X., Cai, X. et al. (2019). Incorporation of rubidium cations into blue perovskite quantum dot light-emitting diodes via FABr-modified multi-cation hot-injection method. *Nanoscale* 11: 1295–1303.

83 Ke, Y., Wang, N., Kong, D. et al. (2019). Defect passivation for red perovskite light-emitting diodes with improved brightness and stability. *The Journal of Physical Chemistry Letters* 10: 380–385.

84 Kovalenko, M.V., Protesescu, L., and Bodnarchuk, M.I. (2017). Properties and potential optoelectronic applications of lead halide perovskite nanocrystals. *Science* 358: 745–750.

85 Kirchartz, T., Markvart, T., Rau, U. et al. (2018). Impact of small phonon energies on the charge-carrier lifetimes in metal-halide perovskites. *The Journal of Physical Chemistry Letters* 9: 939–946.

86 Yang, W.S., Park, B.W., Jung, E.H. et al. (2017). Iodide management in formamidinium-lead-halide-based perovskite layers for efficient solar cells. *Science* 356: 1376–1379.

87 Braly, I.L., deQuilettes, D.W., Pazos-Outón, L.M. et al. (2018). Hybrid perovskite films approaching the radiative limit with over 90% photoluminescence quantum efficiency. *Nature Photonics* 12: 355–361.

88 Yang, X., Zhang, X., Deng, J. et al. (2018). Efficient green light-emitting diodes based on quasi-two-dimensional composition and phase engineered perovskite with surface passivation. *Nature Communications* 9: 570.

89 deQuilettes, D.W., Koch, S., Burke, S. et al. (2016). Photoluminescence lifetimes exceeding 8 μs and quantum yields exceeding 30% in hybrid perovskite thin films by ligand passivation. *ACS Energy Letters* 1: 438–444.

90 Sadaf, S.M., Ra, Y.H., Nguyen, H.P.T. et al. (2015). Alternating-current InGaN/GaN tunnel junction nanowire white-light emitting diodes. *Nano Letters* 15: 6696–6701.

91 Brenes, R., Eames, C., Bulovic, V. et al. (2018). The impact of atmosphere on the local luminescence properties of metal halide perovskite grains. *Advanced Materials* 30: 1706208.

92 Weidman, M.C., Seitz, M., Stranks, S.D. et al. (2016). Highly tunable colloidal perovskite nanoplatelets through variable cation, metal, and halide composition. *ACS Nano* 10: 7830–7839.

93 Tvingstedt, K., Malinkiewicz, O., Baumann, A. et al. (2014). Radiative efficiency of lead iodide based perovskite solar cells. *Scientific Reports* 4: 6071.

94 Chen, C., Gao, L., Gao, W. et al. (1927). Circularly polarized light detection using chiral hybrid perovskite. *Nature Communications* 2019: 10.

95 Wolff, C.M., Zu, F., Paulke, A. et al. (2017). Reduced interface-mediated recombination for high open-circuit voltages in $CH_3NH_3PbI_3$ solar cells. *Advanced Materials* 29: 1700159.

96 Zhang, L., Yang, X., Jiang, Q. et al. (2017). Ultra-bright and highly efficient inorganic based perovskite light-emitting diodes. *Nature Communications* 8: 15640.

97 Wang, J., Wang, N., Jin, Y. et al. (2015). Interfacial control toward efficient and low-voltage perovskite light-emitting diodes. *Advanced Materials* 27: 2311–2316.

98 Lee, S., Park, J.H., Lee, B.R. et al. (2017). Amine-based passivating materials for enhanced optical properties and performance of organic-inorganic perovskites in light-emitting diodes. *The Journal of Physical Chemistry Letters* 8: 1784–1792.

99 Wu, C.Y., Wang, Z., Liang, L. et al. (2019). Graphene-assisted growth of patterned perovskite films for sensitive light detector and optical image sensor application. *Small* 15: 1900730.

100 Hoye, R.L., Chua, M.R., Musselman, K.P. et al. (2015). Enhanced performance in fluorene-free organometal halide perovskite light-emitting diodes using tunable, low electron affinity oxide electron injectors. *Advanced Materials* 27: 1414–1419.

101 Hoye, R.L., Munoz-Rojas, D., Musselman, K.P. et al. (2015). Synthesis and modeling of uniform complex metal oxides by close-proximity atmospheric pressure chemical vapor deposition. *ACS Applied Materials & Interfaces* 7: 10684–10694.

102 Kim, Y.H., Cho, H., Heo, J.H. et al. (2015). Multicolored organic/inorganic hybrid perovskite light-emitting diodes. *Advanced Materials* 27: 1248–1254.

103 Kim, Y.H., Cho, H., and Lee, T.W. (2016). Metal halide perovskite light emitters. *PNAS* 113: 11694–11702.

104 Hoye, R.L.Z., Schulz, P., Schelhas, L.T. et al. (2017). Perovskite-inspired photovoltaic materials: toward best practices in materials characterization and calculations. *Chemistry of Materials* 29: 1964–1988.

105 Brown, T.M., Kim, J.S., Friend, R.H. et al. (1999). Built-in field electroabsorption spectroscopy of polymer light-emitting diodes incorporating a doped poly(3, 4-ethylene-dioxythiophene) hole injection layer. *Applied Physics Letters* 75: 1679–1681.

106 Ziffer, M.E., Mohammed, J.C., and Ginger, D.S. (2016). Electroabsorption spectroscopy measurements of the exciton binding energy, electron-hole reduced effective mass, and band gap in the perovskite $CH_3NH_3PbI_3$. *ACS Photonics* 3: 1060–1068.

107 Amerling, E., Baniya, S., Lafalce, E. et al. (2017). Electroabsorption spectroscopy studies of $(C_4H_9NH_3)_2PbI_4$ organic-inorganic hybrid perovskite multiple quantum wells. *The Journal of Physical Chemistry Letters* 8: 4557–4564.

108 Campbell, I.H., Hagler, T.W., Smith, D.L. et al. (1900). Direct measurement of conjugated polymer electronic excitation energies using metal/polymer/metal structures. *Physical Review Letters* 1996: 76.

109 Cho, C., Zhao, B., Tainter, G.D. et al. (2020). The role of photon recycling in perovskite light-emitting diodes. *Nature Communications* 11: 611.

110 Song, J., Li, J., Li, X. et al. (2015). Quantum dot light-emitting diodes based on inorganic perovskite cesium lead halides ($CsPbX_3$). *Advanced Materials* 27: 7162–7167.

111 Lu, M., Zhang, X., Zhang, Y. et al. (2018). Simultaneous strontium doping and chlorine surface passivation improve luminescence intensity and stability of $CsPbI_3$ nanocrystals enabling efficient light-emitting devices. *Advanced Materials* 30: 1804691.

112 Song, J., Fang, T., Li, J. et al. (2018). Organic-inorganic hybrid passivation enables perovskite QLEDs with an EQE of 16.48%. *Advanced Materials* 30: 1805409.

113 Chiba, T., Hayashi, Y., Ebe, H. et al. (2018). Anion-exchange red perovskite quantum dots with ammonium iodine salts for highly efficient light-emitting devices. *Nature Photonics* 12: 681–687.

114 Hou, S., Gangishetty, M.K., Quan, Q. et al. (2018). Efficient blue and white perovskite light-emitting diodes via manganese doping. *Joule* 2: 2421–2433.

115 Li, J., Duan, C., Zhang, Q. et al. (2023). Self-generated buried submicrocavities for high-performance near-infrared perovskite light-emitting diode. *Nano-Micro Letters* 15: 125.

116 Chen, Z., Li, Z., Chen, Z. et al. (2021). Utilization of trapped optical modes for white perovskite light-emitting diodes with efficiency over 12%. *Joule* 5: 456–466.

117 Bai, W., Xuan, T., Zhao, H. et al. (2023). Perovskite light-emitting diodes with an external quantum efficiency exceeding 30%. *Advanced Materials* 2302283.

118 Zhou, W., Shen, Y., Cao, L.X. et al. (2023). Manipulating ionic behavior with bifunctional additives for efficient sky-blue perovskite light-emitting diodes. *Advanced Functional Materials* 33: 2301425.

119 Jiang, J., Chu, Z., Yin, Z. et al. (2022). Red perovskite light-emitting diodes with efficiency exceeding 25% realized by co-spacer cations. *Advanced Materials* 34: 2204460.

120 Wang, Z., Zheng, S., Teng, Q. et al. (2023). Opportunity of lead-free metal halide perovskites for electroluminescence. *The Innovation Materials* 1: 100015.

121 Tsai, H., Nie, W., Blancon, J.C. et al. (2018). Stable light-emitting diodes using phase-pure Ruddlesden–Popper layered perovskites. *Advanced Materials* 30: 1704217.

122 Yuan, Y. and Huang, J. (2016). Ion migration in organometal trihalide perovskite and its impact on photovoltaic efficiency and stability. *Accounts of Chemical Research* 49: 286–293.

123 Zou, W., Li, R., Zhang, S. et al. (2018). Minimising efficiency roll-off in high-brightness perovskite light-emitting diodes. *Nature Communications* 9: 608.